

Poly(Ethylene Piperidinium)s for Anion Exchange Membranes

Yoonseob Kim (✉ yoonseobkim@ust.hk)

HKUST

Huanhuan Chen

Ye Tian

Chuan Hu

Ran Tao

Yufei Yuan

Rui Wang

Dong-Myeong Shin

Minhua Shao

Young Moo Lee

Research Article

Keywords: Anion exchange membrane, Piperidinium, Polyethylene, Ring-opening metathesis polymerization, Ionic crosslinking

Posted Date: June 21st, 2023

DOI: <https://doi.org/10.21203/rs.3.rs-3078299/v1>

License:   This work is licensed under a Creative Commons Attribution 4.0 International License.

[Read Full License](#)

Abstract

The lack of anion exchange membranes (AEMs) that possess both high hydroxide conductivity and stable mechanical and chemical properties poses a major challenge to the development of high-performance fuel cells. Improving one side of the balance between conductivity and stability usually means sacrificing the other. Herein, we used facile, high-yield chemical reactions to design and synthesize a piperidinium polymer with a polyethylene backbone for AEM fuel cell applications. To improve the performance, we introduced ionic crosslinking into high-cationic-ratio AEMs, PEP80-20PS, to suppress high water uptake and swelling while further improving the hydroxide conductivity. Remarkably, PEP80-20PS achieved a hydroxide conductivity of 354.3 mS cm^{-1} at 80°C while remaining mechanically stable. Compared with the base polymer PEP80, the water uptake and swelling rates of the ionically crosslinked sample at 80°C decreased substantially by 69% and 85%, respectively. PEP80-20PS also showed excellent alkaline stability, 84.7% remained after 35 days of treatment with an aqueous KOH solution. The chemical design in this study represents a significant advancement toward the development of simultaneously highly stable and conductive AEMs for fuel cell applications.

Full Text

Hydrogen energy is a promising option for achieving carbon neutrality, with advantages in terms of near-zero greenhouse gas emissions, renewability, and a bountiful supply. Hydrogen fuel cells efficiently transfer chemical energy from hydrogen to electricity, producing water as a byproduct. Due to their high proton conductivity and long durability, proton-exchange membrane fuel cells (PEMFCs) have been used commercially for years. However, the high cost and vulnerability of the catalysts and expensive membranes used in these fuel cells have hindered the broad industrial adoption of this technology. Comprehensive research has been conducted on anion exchange membrane (AEM) fuel cells (AEMFCs), wherein hydroxides are associated with redox reactions at both electrodes; these fuel cells are compatible with economically feasible catalysts and thus represent a promising new direction.¹

The performance of an AEM is determined by the structure and design of its backbone and cationic moieties. The first generation of AEMs containing ether backbones yielded decent levels of electrochemical performance.² However, their use has declined due to the alkaline instability of the ether bonds. The ether backbones accordingly have been replaced by alkaline-stable, ether-free polymers such as polyethylenes (PEs) and polyarylenes.³ As the alkaline stability of cationic groups is crucial to the ion exchange capacity (IEC; i.e., conductivity and cell power output) of an AEM, a series of cationic groups, including quaternary ammonium,⁴ quaternary phosphonium,⁵⁻⁷ metallocene,⁸ imidazolium,^{9,10} and piperidiniums,¹¹⁻¹³ have been developed and studied. Quaternized ammoniums have become popular because they are easier to synthesize, although their stability is sometimes uncertain. Phosphoniums with bulky groups such as cyclohexane and benzene have also been studied, as their substituents can provide steric hindrance.^{5,7,14} Noonan et al. evaluated the use of the tetrakis(dialkylamino)phosphonium cation in AEMs and observed only a small loss of conductivity from 22 to 18 mS cm^{-1} during an alkaline

stability test.⁵ Furthermore, cobaltocenium-embedded polybenzimidazole AEMs were shown to be stable when electron-donating groups were installed.¹⁵ A cobaltocenium-containing polybenzimidazole membrane prepared via a microwave reaction showed a conductivity loss of 15–20% under the conditions of 1 M KOH and 60°C for 672 h. Substitution of the C2, C4 and C5 positions in imidazolium improved the alkaline stability of this compound significantly by suppressing ring-opening degradation.¹⁶ Wright et al. rationally designed and synthesized imidazolium-based AEMs with a poly(benzimidazole) backbone and steric protection of the C2 position of the benzimidazoliums in the backbone. In these AEMs, C4 and C5 were fused to a benzene ring to further improve the durability.¹⁷

Of the existing cationic groups, piperidiniums (i.e., cyclic quaternary ammoniums) have shown outstanding alkaline stability because a high transition state energy is needed for ring distortion.¹⁸ Thus, piperidiniums cannot be easily degraded via the two main mechanisms of quaternary ammonium degradation: nucleophilic substitution and beta elimination. The installation of piperidiniums on the polyarylene backbones through facile Friedel–Crafts polymerizations has made a significant impact on the development of AEMs.^{11–13} Dozens of studies on linear, pendant and crosslinked poly(aryl piperidiniums) have been published, and all have exhibited the highest level of alkaline stability due to the inclusion of highly stable piperidiniums and ether-free backbones. However, the installation of benzyl groups in piperidiniums facilitates the degradation of these compounds. Marino and Kreuer showed that the half-lives of *N,N*-dimethylpiperidinium and *N*-benzyl-*N*-methylpiperidinium were 87.3 and 7.3 hours, respectively, under the same test conditions (10 mol L⁻¹, 160 °C).¹⁹ *Thus, logic suggests that the most durable piperidinium-based AEMs should be aromatic ring-free; accordingly, PEs are ideal backbones.* To achieve this, ring-opening metathesis polymerization (ROMP) is the most viable option. Although Ziegler–Natta polymerization is possible, its less diverse monomer scope limits product design. Cyclooctadiene derivatives are commonly used as ROMP monomers to prepare PE-based AEMs due to their versatility in forming various cations. Upon hydrogenation, the polymerized products possess a homogeneous C–C-only polyethylene backbone that is chemically stable, mechanically durable and elastic.

Coates and colleagues have led the development of ROMP-enabled PE-based AEMs from cyclooctene derivatives.^{20,21} The conductivity of tetraalkyl ammonium-functionalized PE-based AEMs was comparable to that of Nafion-112.²⁰ Recently, You et al. synthesized the first piperidinium-functionalized PE-based AEM using piperidinium-functionalized cyclooctene.⁴ To prepare (*Z*)-1-(cyclooct-4-en-1-yl)piperidine, the authors of that study used an efficient strategy of hydroamination between inactive olefins and secondary alkyl amines that was photo-catalyzed by [Ir(dF(Me)ppy)₂(dtbbpy)]PF₆, as reported by Musacchio et al.²² The designs of these piperidinium–cyclooctene monomers and the resulting polymers are inventive. However, their AEMs have only yielded decent performances, with hydroxide conductivities of 74–95 mS cm⁻¹ at 80 °C, presumably due to a low IEC (< 1.6 mmol g⁻¹). A low IEC may be a reasonable decision, as a high IEC (usually > 2.5) can result in excessive swelling and mechanical instability. In this work, we designed an improved polymer architecture wherein piperidinium-based PE AEMs have a high IEC of 4.38 mmol g⁻¹, resulting in an exceptionally high conductivity of 354.26 ±

159.35 mS cm⁻¹ at 80 °C while minimizing swelling (< 50%). We installed *N*-methylpiperidinium on the C3 position of 1,5-cyclooctadiene (COD) through a facile substitution reaction between 3-bromocycloocta-1,5-diene and piperidine, followed by a high-yield Menshutkin reaction. These reaction schemes have the advantages of being catalyst-free and economical, producing high yields (> 70% for the three-step process of synthesizing piperidinium-COD from commercial COD). Membranes with such a high IEC and conductivity are often mechanically unstable. Thus, we stabilized these membranes by using both covalent and ionic crosslinking.² Overall, the crosslinked AEMs that contained a high fraction of piperidiniums on the PE backbone showed prolonged mechanical and chemical stability and maintained a high level of conductivity.

We first synthesized monomer **1** from 1,5-cyclooctadiene using an economical and straightforward three-step route (see Fig. 1 and SI for details). The bromination of COD was conducted using *N*-bromosuccinimide (NBS) as the bromine source and azobisisobutyronitrile as the catalyst. Then, we realized C–N coupling via a simple K₂CO₃-assisted nucleophilic substitution between the brominated COD and piperidine. Finally, quaternization by iodomethane yielded the final cationic monomer **1**. Crosslinker **2** was synthesized via a high-yield Grignard reaction between MgBr-COD and Br-COD with a 71% yield. For polymerization, we used a common ROMP condition: the monomers (1 mol L⁻¹; **1** and **2**, 4:1 eq.) and a Grubbs 2nd generation catalyst (1 mmol L⁻¹) were mixed in DCM and stirred at room temperature for 18 hours to produce poly(ethylene piperidinium) (PEP80; the number in the name shows the percentage of **1** in the polymer), an elastic off-white compound, with a yield of 82% (The reaction was characterized by FTIR, Fig. S1). Due to the ionic nature of the polymer, we used a viscometer instead of gel permeation chromatography to characterize the molecular weight. The uncrosslinked base polymer, PEP100, had a high viscosity of 1.92 d L g⁻¹ in DMSO. During ROMP, polymerization occurs through the double bonds at the C5–6 positions. We also synthesized **3** (1-cyclooctene-3-piperidinium) and **4** (two 1-cyclooctenes crosslinked at the C3 position), which have similar structures to **1** and **2** (see the SI and Table S1 and S2), and studied the ROMP activities. However, we could not successfully apply ROMP to monomer **3** despite trying various conditions (monomer concentration, catalyst concentration, temperature; Table S2). Presumably, the bulky piperidinium next to the double bond hindered the coordination between the cycloolefin double bond and metal carbene complex, deactivating the monomer. A similar phenomenon was observed for crosslinker **4** at a relatively low concentration (Table S1).

The optimized PEP80 was prepared systematically. First, we prepared PEP100, a homogeneous polymer. However, its high IEC of 4.48 mmol g⁻¹ and highly soluble nature in water led us to introduce covalent crosslinkers to produce membranes for further characterization. We decreased the percentage of **1** and introduced a crosslinker **2**. The polymer exhibited decreased solubility as the percentage of the crosslinker increased from 5% (PEP95) to 20% (PEP80) and became insoluble in DMF when it reached 25% (PEP75). PEP60 and PEP40 were insoluble in DMF and all other tested solvents, and could not be subjected to hydrogenation or further treatments. We thus used PEP80 with OH⁻ in further studies, unless otherwise noted. For membrane preparation, hydrogenated PEP80 was dissolved in DMF and cast

through slow evaporation at 70 °C, followed by anion exchange in a 1 M KOH aqueous solution overnight. Interestingly, we found that even with 20% crosslinking (PEP80), the membrane with OH⁻ as the counter ion exhibited high water uptake rates of 470% at room temperature and 813% at 80 °C, presumably due to the high percentage of ionic components and the flexible backbone (Fig. 2b). The swelling rate of PEP80 significantly increased from 70–350% when the temperature increased from 20°C to 80 °C. The appearance of the membranes also changed dramatically. When swelled, the PEP80 became nearly colorless and transparent (Fig. S2). Noteworthy, the swelling of PEP80 in 1M KOH solution was reduced to be less than 60% at 80 °C (Fig. S3).

We further stabilized the highly swollen PEP80 by introducing divalent persulfate ions as ionic crosslinkers. We observed that adding a small amount of potassium persulfate (KPS) to the polymer dispersion in deionized (DI) water made the polymer shrink rapidly, yielding an elastic and rubber-like polymer in a solid state (Fig. S4). We conducted an energy-dispersive X-ray (EDX) analysis of thoroughly washed samples and found that sulfur atoms, but not potassium atoms, were observed (Fig. S5). This result indicates the presence of persulfate ions as ionic crosslinkers in the polymer. The increased degree of crosslinking due to persulfates caused PEP80 with 20% PS (percentage about the number of cations on the polymer) to become insoluble in DMF. Then, ionically crosslinked membranes were obtained by hot pressing (see the SI for detailed procedures; hereafter, this sample is noted as PEP80-20PS). According to the piperidinium quantity, PEP80 was treated with 10%, 20% or 30% PS, and the relationships between the ionic crosslinker percentage and membrane properties were investigated. The three samples with different percentages of PS exhibited significant improvements in dimension stability. Water uptake decreased with the addition of the ionic crosslinkers. The water uptake rate of PEP80-30PS decreased to 227% at room temperature, and an increase of only 4% in this rate was observed when the temperature was increased to 80 °C (Fig. 2b and Table 1). As the percentage of ionic crosslinkers decreased, their suppressive effect on membrane swelling was weakened. For PEP80-20PS, the water uptake rate was 256% at 80 °C and the swelling rate was 50.2% (Fig. 2b, c and Table 1). Further decreasing the ionic crosslinker (PEP80-10PS) content yielded a water uptake rate of 350% and a swelling rate of 61.2% at 80 °C. These rates represent significant improvements over the water uptake and swelling rates of PEP80, which were 813% and 350% at 80 °C, respectively.

We characterized the mechanical and electrochemical properties of the optimized sample PEP80-20PS and the control samples, namely PEP80, PEP80-10PS and PEP80-30PS. The mechanical properties of AEMs are essential factors in the interfacial stability and long-term operational durability of a fuel cell. Compared with polyarylenes, PEs have remarkable mechanical properties due to their highly flexible, all single-carbon-bond backbones. To measure the mechanical properties, we equilibrated the samples at 20 °C and 60 RH% overnight before taking measurements. Despite the potentially weak bond in a single ionic crosslink, at a high density, the ionic bonds exerted a substantial force on the membranes. Overall, the stress–strain curves of the AEMs show elastic and strong thermoset features due to the high percentage of crosslinking. All four AEMs, namely PEP80, PEP80-10PS, PEP80-20PS and PEP80-30PS, had similar maximum levels of tensile stress around 1 MPa but differences in the maximum tensile stress depending

on the degree of ionic crosslinking (Fig. 2a). AEMs with fewer ionic crosslinkers tended to be more elastic. For PEP80-30PS, the tensile strain required for membrane failure was only 130%. However, for PEP80-10PS, which contained fewer ionic crosslinkers, the maximum tensile strain increased to 210%. By contrast, PEP80 had more flexible features with a strain at the break of 227%. In terms of the thermal stability, PEP80 showed no weight loss until 200 °C, while PEP80-*n*PS lost around 3% of their total weight when the temperature reached 200 °C. The TGA pattern of the AEMs confirmed its thermal stability in fuel cell's working temperature (Fig. S6).

Following the investigation and optimization of the membranes, we measured the hydroxide conductivity of PEP80, PEP80-10PS, PEP80-20PS and PEP80-30PS over a temperature range of 20–80 °C at intervals of 10 °C. Introducing ionic crosslinkers improved not only the water uptake and dimensional stability of the AEMs but also their hydroxide conductivity. PEP80-20PS exhibited the highest hydroxide conductivities of 354.3 mS cm⁻¹ at 80 °C and 55.9 mS cm⁻¹ at 20 °C (Fig. 3). Although the performances of PEP80-10PS and PEP80-30PS were slightly lower than that of PEP80-20PS, both membranes exhibited excellent performance compared with most published AEMs, with conductivities of 147.7 and 204.7 mS cm⁻¹ at 80 °C, respectively. When the temperature was lowered to 60 °C, the conductivity of PEP80-20PS remained high at 167.9 mS cm⁻¹, while those of PEP80-10PS and PEP80-30PS were appreciably lower at 87.2 and 110.0 mS cm⁻¹, respectively. To the best of our knowledge, the conductivity of PEP80-20PS at 80 °C, 354.3 mS cm⁻¹, is almost double the previously recorded maximum value.²⁴

The observed conductivities above 85 mS cm⁻¹ over the temperature range of 60–80 °C, i.e., the working temperatures of fuel cells, proved well the usability of these AEMs. Overall, PEP80-20PS had the best conductivity among the three samples. Compared with PEP80-30PS, the less numerous cationic sites in PEP80-20PS were occupied by persulfate ions and thus made a greater contribution to OH⁻ transport. The water uptake of PEP80-10PS was significantly higher than that of PEP80-20PS, especially under elevated temperatures (a difference of 37% at 80 °C), which reduced its conductivity. In addition, ion crosslinked PEP80 membranes (PEP80-*n*PS) revealed much more stable behavior than PEP80. The Arrhenius equation is well suited to describe the temperature-dependent hydroxide conductivity of PEP80-*n*PS. According to this equation, the activation energies of PEP80-10PS, PEP80-20PS and PEP80-30PS were very similar, with respective values of 27.0, 26.2 and 26.8 kJ mol⁻¹ (Fig. S7). The conductivity of these crosslinked membrane samples varied at higher temperatures, indicating that ionic crosslinking may not be fully stable under such thermal conditions. Finally, we measured the alkaline stabilities of the AEMs after treating them with 1 M KOH solution at 80 °C for up to 35 days. The changes in conductivity were measured and normalized to the initial conductivity measured during the alkaline stability test. All of the samples exhibited a stable performance under the test condition. Specifically, PEP80-30PS, PEP80-20PS, PEP80-10PS and PEP80 retained 87.5%, 84.7%, 81.3% and 75.4% of their initial conductivities, respectively (Fig. 3b). The conductivities of all three AEM samples were enhanced after one day of alkaline treatment but then decreased over the remaining testing period. One possible reason for the initial increase in conductivity is that some of the ionic crosslinkers were exchanged for OH⁻ ions. For the

piperidinium-functionalized AEMs, cation degradation through both Hofmann elimination and nucleophilic substitution is the main cause of the disablement of cations and loss of conductivity.⁴

In conclusion, we synthesized a piperidinium monomer based on cyclooctadiene via facile economical reactions and prepared a cationic polymer using highly efficient ROMP. We obtained a series of piperidinium-functionalized AEMs with various ionic crosslinking ratios and systematically studied their properties. The ionically crosslinked AEMs achieved a balance between a high IEC (high conductivity) and limited dimensional change. We found that the introduction of ionic crosslinkers not only improved the mechanical stability of the AEMs but also promoted their hydroxide conductivity. PEP80-20PS achieved an all-time high conductivity of 354.3 mS cm^{-1} at $80 \text{ }^\circ\text{C}$. All of the ionically crosslinked AEMs showed excellent alkaline stability, with approximately 84.7% of conductivity remaining after 35 days of exposure to alkaline conditions. However, it was difficult to prepare a macro-scale defect-free membrane for fuel cell tests due to the thermoset nature of the ionically crosslinked AEMs. Further research efforts to optimize engineering are needed.

Declarations

Acknowledgment

This work was supported by the Research Grants Council of the Hong Kong SAR Government (Early Career Scheme, #26309420, General Research Fund, #16306921 and #16306022, and Collaborative Research Fund, #C6011-20G), the Department of Chemical and Biomolecular Engineering, HKUST (startup funding) and the 30 for 30 Research Initiative Scheme, VPRDO, HKUST.

Conflict of Interest

The authors declare no conflicts of interest.

References

1. You, W.; Noonan, K. J. T.; Coates, G. W. Alkaline-Stable Anion Exchange Membranes: A Review of Synthetic Approaches. *Prog. Polym. Sci.* **2020**, *100*, 101177.
2. Kim, Y.; Wang, Y.; France-Lanord, A.; Wang, Y.; Wu, Y. C. M.; Lin, S.; Li, Y.; Grossman, J. C.; Swager, T. M. Ionic Highways from Covalent Assembly in Highly Conducting and Stable Anion Exchange Membrane Fuel Cells. *J. Am. Chem. Soc.* **2019**, *141*, 45, 18152–18159.
3. Chen, H.; Tao, R.; Bang, K. T.; Shao, M.; Kim, Y. Anion Exchange Membranes for Fuel Cells: State-of-the-Art and Perspectives. *Adv. Energy Mater.* **2022**, *12*, 28, 1–11.
4. You, W.; Ganley, J. M.; Ernst, B. G.; Peltier, C. R.; Ko, H. Y.; DiStasio, R. A.; Knowles, R. R.; Coates, G. W. Expedient Synthesis of Aromatic-Free Piperidinium-Functionalized Polyethylene as Alkaline Anion Exchange Membranes. *Chem. Sci.* **2021**, *12*, 11, 3898–3910.

5. Noonan, K. J. T.; Hugar, K. M.; Kostalik, H. A.; Lobkovsky, E. B.; Abruña, H. D.; Coates, G. W. Phosphonium-Functionalized Polyethylene: A New Class of Base-Stable Alkaline Anion Exchange Membranes. *J. Am. Chem. Soc.* **2012**, *134*, 44, 18161–18164.
6. Han, H.; Ma, H.; Yu, J.; Zhu, H.; Wang, Z. Preparation and Performance of Novel Tetraphenylphosphonium-Functionalized Polyphosphazene Membranes for Alkaline Fuel Cells. *Eur. Polym. J.* **2019**, *114*, February, 109–117.
7. Tao, Z.; Wang, C.; Zhao, X.; Li, J.; Guiver, M. D. Progress in High-Performance Anion Exchange Membranes Based on the Design of Stable Cations for Alkaline Fuel Cells. *Adv. Mater. Technol.* **2021**, *6*, 5, 1–14.
8. Zhu, T.; Xu, S.; Rahman, A.; Dogdibegovic, E.; Yang, P.; Pageni, P.; Kabir, M. P.; Zhou, X. D.; Tang, C. Cationic Metallo-Polyelectrolytes for Robust Alkaline Anion-Exchange Membranes. *Angew. Chemie - Int. Ed.* **2018**, *57*, 9, 2388–2392.
9. You, W.; Hugar, K. M.; Coates, G. W. Synthesis of Alkaline Anion Exchange Membranes with Chemically Stable Imidazolium Cations: Unexpected Cross-Linked Macrocycles from Ring-Fused ROMP Monomers. *Macromolecules* **2018**, *51*, 8, 3212–3218.
10. You, W.; Padgett, E.; MacMillan, S. N.; Muller, D. A.; Coates, G. W. Highly Conductive and Chemically Stable Alkaline Anion Exchange Membranes via ROMP of Trans-Cyclooctene Derivatives. *Proc. Natl. Acad. Sci. U. S. A.* **2019**, *116*, 20, 9729–9734.
11. Wang, J.; Zhao, Y.; Setzler, B. P.; Rojas-Carbonell, S.; Ben Yehuda, C.; Amel, A.; Page, M.; Wang, L.; Hu, K.; Shi, L.; Gottesfeld, S.; Xu, B.; Yan, Y. Poly(Aryl Piperidinium) Membranes and Ionomers for Hydroxide Exchange Membrane Fuel Cells. *Nat. Energy* **2019**, *4*, 392–398.
12. Chen, N.; Hu, C.; Wang, H. H.; Kim, S. P.; Kim, H. M.; Lee, W. H.; Bae, J. Y.; Park, J. H.; Lee, Y. M. Poly(Alkyl-Terphenyl Piperidinium) Ionomers and Membranes with an Outstanding Alkaline-Membrane Fuel-Cell Performance of 2.58 W Cm⁻². *Angew. Chemie - Int. Ed.* **2021**, *60*, 14, 7710–7718.
13. Chen, N.; Wang, H. H.; Kim, S. P.; Kim, H. M.; Lee, W. H.; Hu, C.; Bae, J. Y.; Sim, E. S.; Chung, Y. C.; Jang, J. H.; Yoo, S. J.; Zhuang, Y.; Lee, Y. M. Poly(Fluorenyl Aryl Piperidinium) Membranes and Ionomers for Anion Exchange Membrane Fuel Cells. *Nat. Commun.* **2021**, *12*, 2367.
14. Womble, C. T.; Coates, G. W.; Matyjaszewski, K.; Noonan, K. J. T. Tetrakis(Dialkylamino)Phosphonium Polyelectrolytes Prepared by Reversible Addition-Fragmentation Chain Transfer Polymerization. *ACS Macro Lett.* **2016**, *5*, 2, 253–257.
15. Chen, N.; Zhu, H.; Chu, Y.; Li, R.; Liu, Y.; Wang, F. Cobaltocenium-Containing Polybenzimidazole Polymers for Alkaline Anion Exchange Membrane Applications. *Polym. Chem.* **2017**, *8*, 8, 1381–1392.
16. Hugar, K. M.; Kostalik, H. A.; Coates, G. W. Imidazolium Cations with Exceptional Alkaline Stability: A Systematic Study of Structure-Stability Relationships. *J. Am. Chem. Soc.* **2015**, *137*, 27, 8730–8737.
17. Ionen, H.; Wright, A. G.; Holdcroft, S. Hydroxide-Stable Ionen. **2014**, 444–447.

18. Olsson, J. S.; Pham, T. H.; Jannasch, P. Poly(Arylene Piperidinium) Hydroxide Ion Exchange Membranes: Synthesis, Alkaline Stability, and Conductivity. *Adv. Funct. Mater.* **2018**, *28*, 2, 1–10.
19. Marino, M. G.; Kreuer, K. D. Alkaline Stability of Quaternary Ammonium Cations for Alkaline Fuel Cell Membranes and Ionic Liquids. *ChemSusChem* **2015**, *8*, 3, 513–523.
20. Robertson, N. J.; Kostalik IV, H. A.; Clark, T. J.; Mutolo, P. F.; Abruña, H. D.; Coates, G. W. Tunable High Performance Cross-Linked Alkaline Anion Exchange Membranes for Fuel Cell Applications. *J. Am. Chem. Soc.* **2010**, *132*, 10, 3400–3404.
21. Kostalik, H. A.; Clark, T. J.; Robertson, N. J.; Mutolo, P. F.; Longo, J. M.; Abruña, H. D.; Coates, G. W. Solvent Processable Tetraalkylammonium-Functionalized Polyethylene for Use as an Alkaline Anion Exchange Membrane. *Macromolecules* **2010**, *43*, 17, 7147–7150.
22. Musacchio, A. J.; Lainhart, B. C.; Zhang, X.; Naguib, S. G.; Sherwood, T. C.; Knowles, R. R. Catalytic Intermolecular Hydroaminations of Unactivated Olefins with Secondary Alkyl Amines. *Science (80-)*. **2017**, *355*, 6326, 727–730.
23. Mayadevi, T. S.; Sung, S.; Varghese, L.; Kim, T. H. Poly(Meta/Para-Terphenylene-Methyl Piperidinium)-Based Anion Exchange Membranes: The Effect of Backbone Structure in Aemfc Application. *Membranes (Basel)*. **2020**, *10*, 11, 1–16.
24. Yuan, W.; Zeng, L.; Jiang, S.; Yuan, C.; He, Q.; Wang, J.; Liao, Q.; Wei, Z. High Performance Poly(Carbazolyl Aryl Piperidinium) Anion Exchange Membranes for Alkaline Fuel Cells. *J. Memb. Sci.* **2022**, *657*, April, 120676.
25. Wang, H. H.; Hu, C.; Park, J. H.; Kim, H. M.; Kang, N. Y.; Bae, J. Y.; Lee, W. H.; Chen, N.; Lee, Y. M. Reinforced Poly(Fluorenyl-Co-Terphenyl Piperidinium) Anion Exchange Membranes for Fuel Cells. *J. Memb. Sci.* **2022**, *644*, September 2021, 120160.
26. Hu, C.; Park, J. H.; Kim, H. M.; Wang, H. H.; Bae, J. Y.; Kang, N. Y.; Chen, N.; Lee, Y. M. Elucidating the Role of Alkyl Chain in Poly(Aryl Piperidinium) Copolymers for Anion Exchange Membrane Fuel Cells. *J. Memb. Sci.* **2022**, *647*, January, 120341.
27. Liu, L.; Bai, L.; Liu, Z.; Miao, S.; Pan, J.; Shen, L.; Shi, Y.; Li, N. Side-Chain Structural Engineering on Poly(Terphenyl Piperidinium) Anion Exchange Membrane for Water Electrolysers. *J. Memb. Sci.* **2023**, *665*, October 2022, 121135.
28. Yang, Y.; Jiang, T.; Li, L.; Zhou, S.; Fang, H.; Li, X.; Wei, H.; Ding, Y. Chemo-Stable Poly(Quinquephenylene-Co-Diphenylene Piperidinium) Ionomers for Anion Exchange Membrane Fuel Cells. *J. Power Sources* **2021**, *506*, June, 230184.
29. Gao, W. T.; Gao, X. L.; Gou, W. W.; Wang, J. J.; Cai, Z. H.; Zhang, Q. G.; Zhu, A. M.; Liu, Q. L. High-Performance Tetracyclic Aromatic Anion Exchange Membranes Containing Twisted Binaphthyl for Fuel Cells. *J. Memb. Sci.* **2022**, *655*, April, 120578.
30. Hu, C.; Park, J. H.; Kim, H. M.; Wang, H. H.; Bae, J. Y.; Liu, M. L.; Kang, N. Y.; Yoon, K. S.; Park, C. D.; Chen, N.; Lee, Y. M. Robust and Durable Poly(Aryl-Co-Aryl Piperidinium) Reinforced Membranes for Alkaline Membrane Fuel Cells. *J. Mater. Chem. A* **2022**, *10*, 12, 6587–6595.

31. Cai, Z. H.; Gao, X. L.; Gao, W. T.; Choo, Y. S. L.; Wang, J. J.; Zhang, Q. G.; Zhu, A. M.; Liu, Q. L. Effect of Hydrophobic Side Chain Length on Poly(Carbazolyl Terphenyl Piperidinium) Anion Exchange Membranes. *ACS Appl. Energy Mater.* **2022**, *5*, 8, 10165–10176.
32. Pan, D.; Bakvand, P. M.; Pham, T. H.; Jannasch, P. Improving Poly(Arylene Piperidinium) Anion Exchange Membranes by Monomer Design. *J. Mater. Chem. A* **2022**, *10*, 31, 16478–16489.
33. Xu, L.; Wang, H.; Min, L.; Xu, W.; Wang, Y.; Zhang, W. Anion Exchange Membranes Based on Poly(Aryl Piperidinium) Containing Both Hydrophilic and Hydrophobic Side Chains. *Ind. Eng. Chem. Res.* **2022**, *61*, 38, 14232–14241.
34. Kim, H. M.; Hu, C.; Wang, H. H.; Park, J. H.; Chen, N.; Lee, Y. M. Impact of Side-Chains in Poly (Dibenzyl-Co-Terphenyl Piperidinium) Copolymers for Anion Exchange Membrane Fuel Cells. *J. Memb. Sci.* **2022**, *644*, September 2021, 120109.
35. Lin, C.; Cheng, W.; Miao, X.; Shen, X.; Ling, L. Clustered Piperidinium-Functionalized Poly(Terphenylene) Anion Exchange Membranes with Well-Developed Conductive Nanochannels. *J. Colloid Interface Sci.* **2022**, *608*, 1247–1256.
36. Ma, L.; Hussain, M.; Li, L.; Qaisrani, N. A.; Bai, L.; Jia, Y.; Yan, X.; Zhang, F.; He, G. Octopus-like Side Chain Grafted Poly(Arylene Piperidinium) Membranes for Fuel Cell Application. *J. Memb. Sci.* **2021**, *636*, January.
37. Gou, W. W.; Gao, W. T.; Gao, X. L.; Zhang, Q. G.; Zhu, A. M.; Liu, Q. L. Highly Conductive Fluorinated Poly(Biphenyl Piperidinium) Anion Exchange Membranes with Robust Durability. *J. Memb. Sci.* **2022**, *645*, December 2021, 120200.
38. Liu, Q.; Ma, W.; Tian, L.; Li, J.; Yang, L.; Wang, F.; Wang, Z.; Li, J.; Wang, Z.; Zhu, H. Side-Chain Cation-Grafted Poly(Biphenyl Piperidine) Membranes for Anion Exchange Membrane Fuel Cells. *J. Power Sources* **2022**, *551*, May, 232105.
39. Allushi, A.; Pham, T. H.; Jannasch, P. Highly Conductive Hydroxide Exchange Membranes Containing Fluorene-Units Tethered with Dual Pairs of Quaternary Piperidinium Cations. *J. Memb. Sci.* **2021**, *632*, December 2020, 119376.
40. Long, C.; Wang, Z.; Zhu, H. High Chemical Stability Anion Exchange Membrane Based on Poly(Aryl Piperidinium): Effect of Monomer Configuration on Membrane Properties. *Int. J. Hydrogen Energy* **2021**, *46*, 35, 18524–18533.
41. Chen, N.; Hu, C.; Wang, H. H.; Park, J. H.; Kim, H. M.; Lee, Y. M. Chemically & Physically Stable Crosslinked Poly(Aryl-Co-Aryl Piperidinium)s for Anion Exchange Membrane Fuel Cells. *J. Memb. Sci.* **2021**, *638*, June, 119685.
42. Min, K.; Chae, J. E.; Lee, Y.; Kim, H. J.; Kim, T. H. Crosslinked Poly(m-Terphenyl N-Methyl Piperidinium)-SEBS Membranes with Aryl-Ether Free and Kinked Backbones as Highly Stable and Conductive Anion Exchange Membranes. *J. Memb. Sci.* **2022**, *653*, January, 120487.
43. Jia, Y.; Ma, L.; Yu, Q.; Qaisrani, N. A.; Li, L.; Zhou, R.; He, G.; Zhang, F. Partially Fluorinated, Multication Cross-Linked Poly(Arylene Piperidinium) Membranes with Improved Conductivity and Reduced Swelling for Fuel Cell Application. *Ionics (Kiel)*. **2020**, *26*, 11, 5617–5627.

44. Du, X.; Zhang, H.; Yuan, Y.; Wang, Z. Constructing Micro-Phase Separation Structure to Improve the Performance of Anion-Exchange Membrane Based on Poly(Aryl Piperidinium) Cross-Linked Membranes. *J. Power Sources* **2021**, *487*, January, 229429.
45. Wang, J. J.; Gao, W. T.; Choo, Y. S. L.; Cai, Z. H.; Zhang, Q. G.; Zhu, A. M.; Liu, Q. L. Highly Conductive Branched Poly(Aryl Piperidinium) Anion Exchange Membranes with Robust Chemical Stability. *J. Colloid Interface Sci.* **2023**, *629*, 377–387.

Table

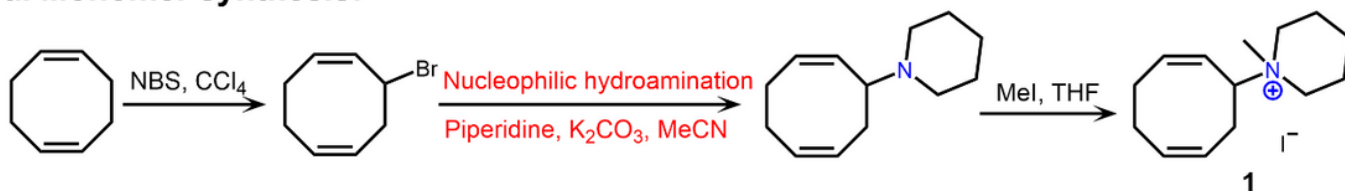
Table 1. Chemical and mechanical properties of the PEP-AEMs.

AEMs	IEC (mmol·g ⁻¹)		WU (%)		SR (%)		σ (mS·cm ⁻¹)	
	Theor.	Titra.	20 °C	80 °C	20 °C	80 °C	20 °C	80 °C
PEP80	4.52	4.38	473	813	70.0	350.0	82	85
PEP80-10PS	/	4.17	297	350	56.1	61.2	23	147
PEP80-20PS	/	4.05	243	256	48.1	50.2	56	354
PEP80-30PS	/	3.70	227	231	38.0	38.5	30	205

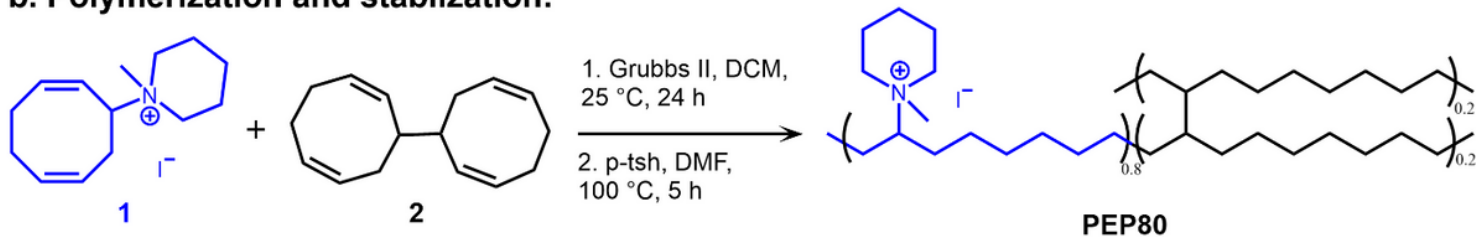
*WU, SR and σ represent the water uptake rate, the swelling rate and hydroxide conductivity, respectively.

Figures

a. Monomer synthesis:



b. Polymerization and stabilization:



c. Membrane stabilization

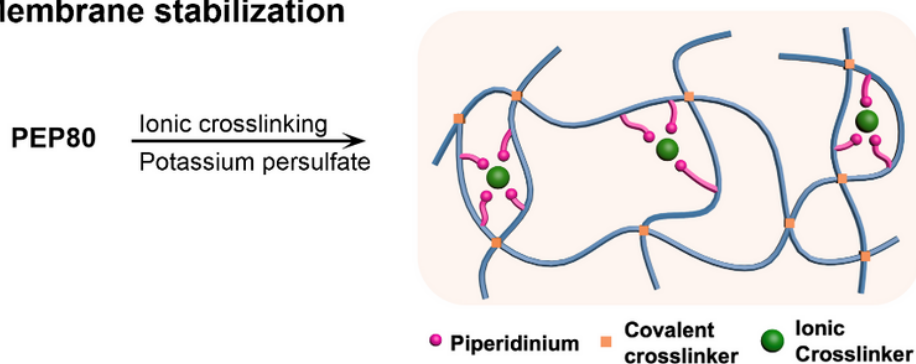


Figure 1

Synthetic route to PEP80 AEMs and schematic of ionic crosslinking. **a**, Three-step synthesis of the piperidinium-functionalized cyclooctadiene monomer. **b**, Synthesis of the polymer through ring-opening metathesis polymerization to form a covalently crosslinked copolymer. Hydrogenation was achieved through diimide reduction. **c**, Illustration of ionic crosslinking of the polymer to further stabilize the AEMs.

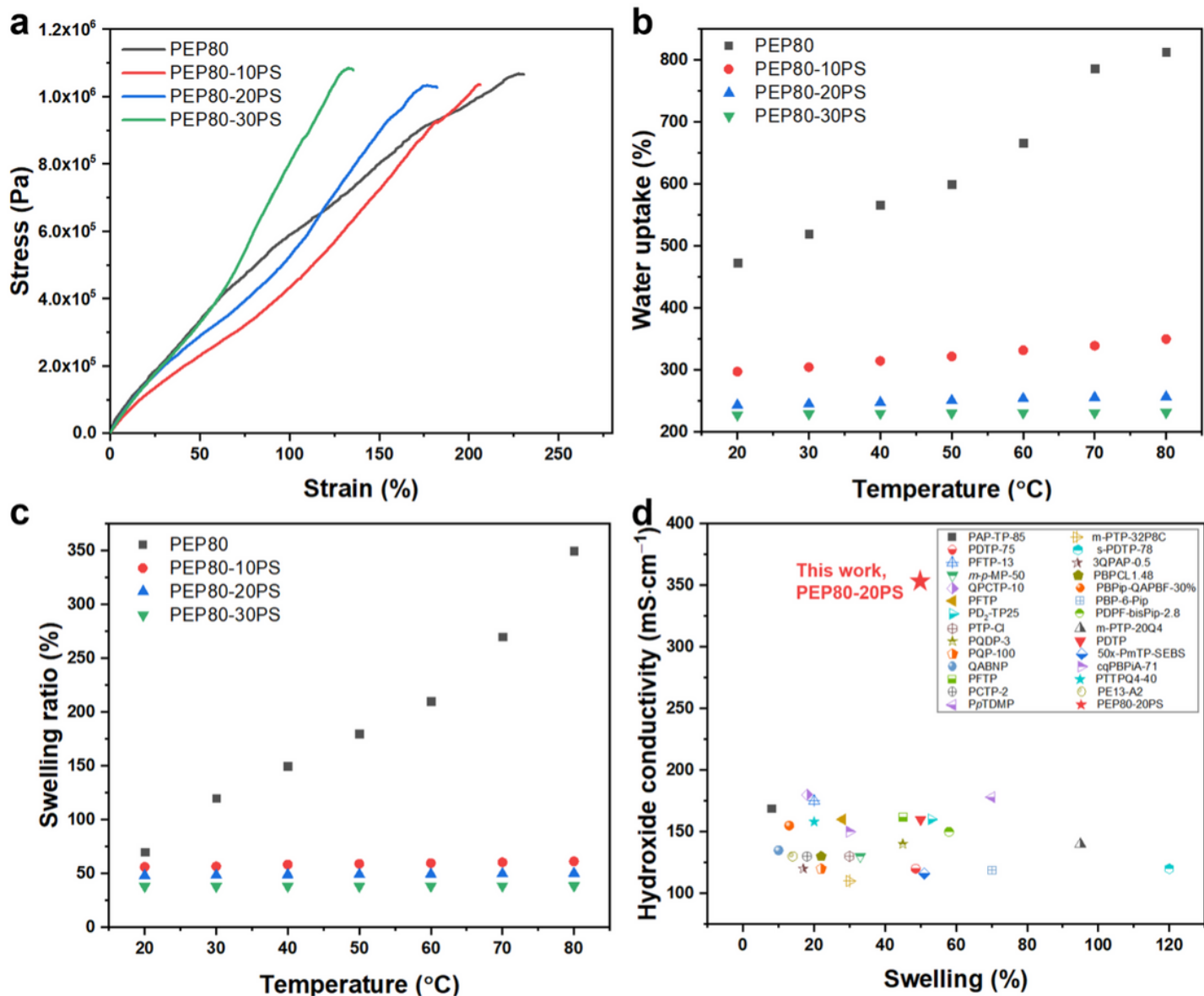


Figure 2

Properties of the PEP-AEMs. **a**, Stress–strain curves of the AEMs. **b, c**, Water uptake and in-plane swelling rates of the AEMs over a temperature range of 20–80 °C, respectively. **d**, Comparison of hydroxide conductivity and swelling rates between this work and other representative AEMs with piperidinium. (References: PAP-TP-85,¹¹ PDTP-75,¹² PFTP-13,¹³ *m-p*-MP-50,²³ QPCTP-10,²⁴ PFTP,²⁵ PD₂-TP25,²⁶ PTP-Cl,²⁷ PQDP-3,²⁸ PQP-100,²³ QABNP²⁹, PFTP³⁰, PCTP-2³¹, P_pTDMP³², m-PTP-32P8C³³, s-PDTP-78³⁴, 3QPAP-0.5³⁵, PBPCL1.48³⁶, PBIP-QAPBF-30%³⁷, PBP-6-Pip³⁸, PDPF-bisPip-2.8³⁹, m-PTP-20Q4⁴⁰, PDTP⁴¹, 50x-PmTP-SEBS⁴², cqPBPIA-71⁴³, PAP-OH-8%⁴⁴, PTPQ4-40⁴⁵.)

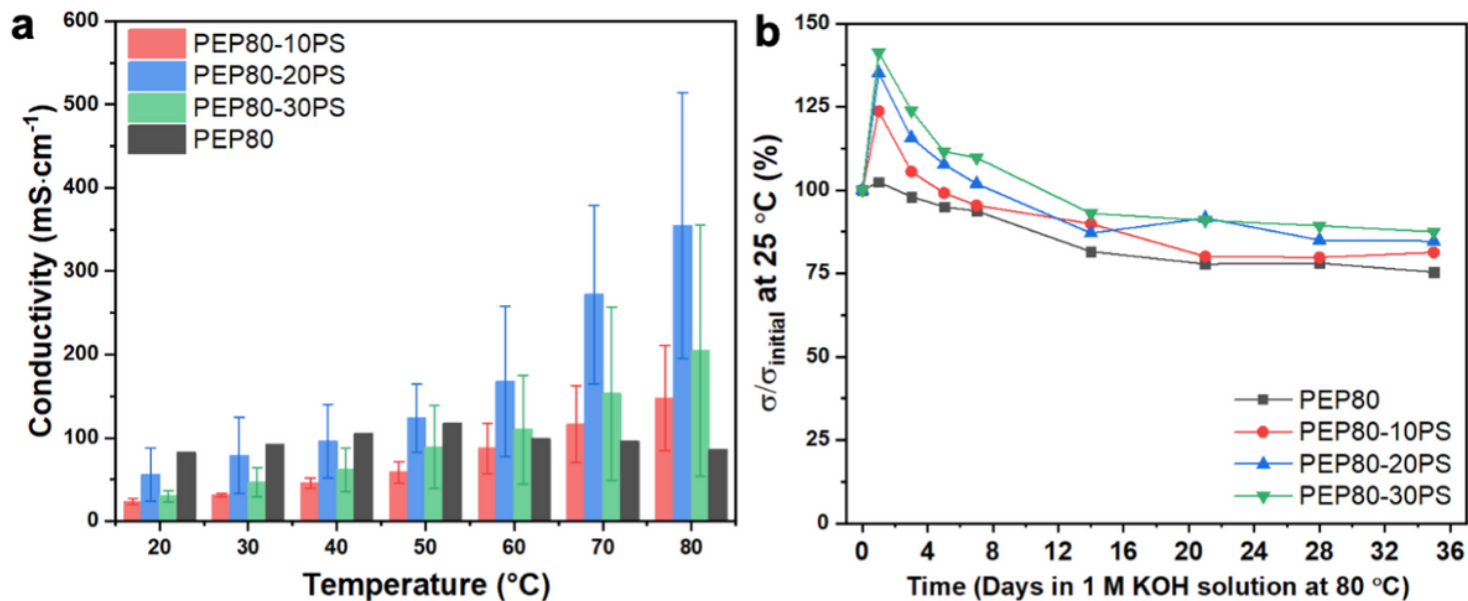


Figure 3

Hydroxide conductivities of the PEP-AEMs. **a**, Hydroxide conductivities of the AEMs. Shown are the averages of nine data points (three data points for each of the three samples) with their standard deviations (error ranges). **b**, Alkaline stability of the AEMs, expressed by the percentage of conductivity remaining, measured at 25 °C.

Supplementary Files

This is a list of supplementary files associated with this preprint. Click to download.

- [PEPSI.docx](#)
- [TOCfigure.docx](#)